GSA DATA REPOSITORY 2020060

Chan, P.T.W., et al., 2020, Recent density decline in wild-collected subarctic crustose coralline algae reveals climate change signature: Geology, v. 48, https://doi.org/10.1130/G46804.1

Supplementary Material

Sample Collection

Live specimens of *Clathromorphum nereostratum* were collected in 2004, and 2008 at 8-10 m water depth via SCUBA off Attu island (N 52° 47.78, E 173° 10.796) and Amchitka island (N 51° 25.568, E 179° 14.277) of the Aleutian archipelago, Alaska (Fig. 1AB). Additional samples live-collected in 1969 were obtained from the University of British Columbia Herbarium and the U.S. National Herbarium Collection at the Smithsonian Institution in Washington D.C.). The microenvironment from which the algae were collected was noted at the time of collection (varying from little to no kelp, to dense kelp cover). The presence of kelp can influence light levels reaching the shallow seafloor. However, the presence and abundance of kelp varies over multidecadal timescales, and historical observation data is not available at the collection sites.

Sample Preparation

Samples were vertically thick-sectioned into 1.5 - 2 cm slabs parallel to the growth axis of the alga and polished to a 3 μm finish. High resolution digital photomosaics of each polished specimen surface was scanned using an Olympus reflected light microscope (VS-BX) attached to an automated sampling stage imaging system equipped with Geo.TS software (Olympus Soft Imaging Systems (for details, see Hetzinger et al., 2009). This microscopic scanning setup enabled detailed viewing with zoom and panning functions using a pyramidal file format. The resulting photomosaics facilitated the establishment of a precise age model through the identification of annual growth increments, which are delineated by couplets of dark and light bands, and coincide with the occurrence of rows of annually forming conceptacles. Conceptacles are uniformly-sized cavities that enclose the algal reproductive structures, and form seasonally in Fall (September – October) by the downward decalcification of skeletal material (Fig. 2A).

Micro-CT Setup

Specimens were scanned in a micro-CT scanner (GE Healthcare, eXplore Locus RS) at a peak x-ray energy of 80 kVp and tube current of 450 uA at a resolution of 20 μm. 900 x-ray projections or views (image matrix size 2010 x 1920 pixels) were collected at 0.4 degree angular increments over a single 360° rotation. Each projection was 4500 ms in duration and 2 image frames were acquired at each view angle and averaged to reduce image noise resulting in a 2.75 hour long scan. Each averaged x-ray projection was corrected for brightfield, darkfield, and geometric distortions and then a 3D volumetric image was reconstructed from the x-ray projection data using a filtered-back projection algorithm with isotropic 20.17 um voxels. Sample vials containing air, water, Hydroxyapatite SB3 cortical bone mimic $Ca_5(PO_4)_3(OH)$, (Gammex RMI, density = 1.83 g/cm^3), and calcite crystal (pure calcium carbonate $CaCO_3$, density = 2.71 g/cm^3) were included in the scanner field of view (FOV) with each sample during

acquisition and used for calibration purposes. The 3D data set was linearly rescaled into Hounsfield units (HU) so that air was represented by voxel greyscale values near -1000 and water by values near 0. Samples roughly the same size as the scanner field of view (FOV) or larger were scanned in multiple sections and digitally concatenated or stitched into a single, larger 3D volume. Samples were oriented such that the CT scan slice-plane was as perpendicular as possible to the growth axis of the coralline algae samples (from young to old).

Micro-CT imaging produced a 3D distribution of linear attenuation coefficients that was stored as an x-ray volume image for each algal specimen, defined by an X-Y in-plane axis, and a Z-axis following the growth axis. Sample visualization and analysis was performed using MicroView Standard 2.5.0–2799 (Parallax Innovations Inc., 2015) to reconstruct the specimen in 3D, and to digitize a region of interest (ROI; delineating the region to be analyzed). The ROI was plotted as a tall, thin, square based prism (on the X-Y plane: 81 X 81 pixels or 1.59 X 1.59 mm) spanning the entire Z- range (axis of algal growth), this ROI was selected for each specimen such that it avoided areas with cracks, boring cavities or diagenetic alterations as much as possible (Fig. 2AB). The ROI was then cropped out from the complete volume, and analyzed on a 20 μm thick slab-by-slab basis perpendicular to the Z-growth axis. Annual growth increments (average 0.03 cm/year) were clearly delineated by couplets of dark and light banding patterns visible in the micro-CT ROI core, and coincide with the occurrence of rows of annually forming conceptacles (randomly distributed black cavities enclosing algal reproductive structures; Fig. 2AB). Ellipsoid-shaped conceptacles are uniformly-sized and randomly distributed in three-dimensional space, hence any particular slice cutting through a number of conceptacles shows conceptacle size variations due to the positioning of the slice through the cavity (e.g. at the edge vs. through the center). A threshold greyscale value of 2400 HU was carefully selected to digitally remove conceptacle cavities (ranging from 150 - 200 μm in diameter) from the skeletal density calculation. This approach assured consistent sampling focused on skeletal calcite only. Voxels with a greyscale value below the threshold were deemed to be empty space and excluded from the skeletal density calculation. However, skeletal porosity was included in the skeletal density calculation as small pore spaces (~ 5 μm) were unresolvable at 20 μm resolution. Skeletal density for each slice (average 1.55 g/cm^3) was determined using the fractional mineral content of each voxel (3D pixel) above the greyscale threshold (to exclude conceptacle cavies), averaged over all the voxels in that slice, and linearly rescaled to units of pure crystal calcite (density = 2.71 g/cm^3). A weighted average was then applied to the density values of all the slices within each annual growth increment to generate the annual skeletal density value for each year of growth. High resolution micro-CT enables sub-annual density determinations, and has shown seasonal variations in *Clathromorphum* related to changes in sunlight and temperature (Chan et al., 2017). Lastly, annual calcification rates (0.05 $g/cm^2/yr$) were calculated as the product of annual growth rates and annual skeletal densities. Please refer to Chan et al., (2017) for detailed methods. Algal growth, skeletal density, and calcification rate measurements from the epithallus (the outer calcified protective layer analogous to the bark of a tree) and the final two years of growth were removed from every sample to avoid inclusion of the youngest growth layers, which may experience incomplete formation and thus exhibit artificial ontogenetic-related declines (D'Olivo et al., 2013; De'ath et al., 2013; Ridd et al., 2013).

Supplementary Tables

Table DR1: Skeletal density line of best fit slope values for recent collected specimens. This table shows slope values for the line of best fit in the last 10, 15, and 20 years of the skeletal density time series in recently collected specimens.

Last years	Attu 11-4	Attu 11-5	AM 4-1	AM 7-6	08-10-25	08-10-28
10	-0.1036	-0.3003	-0.0308	0.0168	-0.0121	-0.3019
15	-0.0997	-0.2482	-0.1735	0.0953	-0.0851	-0.1372
20	-0.1014	-0.2047	-0.1058	0.0497	-0.0958	-0.0930

Table DR2: Skeletal density line of best fit slope values for older collected specimens. This table shows slope values for the line of best fit in the last 10, 15, and 20 years of the skeletal density time series in older collected specimens

Last years	AM-SM-30	AM-OC-70	AM-KP-80
10	0.1620	0.0053	0.2064
15	0.1346	0.0220	0.0422
20	0.1164	-0.0129	0.0360

Table DR3: Statistical tests used to compare the means of the line of best fit slope values in the skeletal density time series for both recent and older collected specimens.

	Shapiro-Wilks		F-test	t-test
Last Years	Modern (*p*-value)	Museum (*p*-value)	F-test (*p*-value)	1 tailed (*p*-value)
10	0.0881	0.4043	0.7691	0.01787
15	0.5733	0.3228	0.4524	0.02377
20	0.1571	0.7331	0.8727	0.01940

A Shapiro-Wilks test (for normality) and an F-test (for homogeneity of variances) was conducted on the slope values of the line of best fit for the last 10, 15, and 20 years of the skeletal density time series in each of the two groups (recent and older collected samples). The tests indicate that the slope values for both recent and older collected samples are normally distributed, and that the two groups have equal variances. Therefore, a one-tailed t-test was performed to determine if the line of best fit slope values for recent collected samples were significantly lower than the line of best fit slope values for older collected samples. The t-test *p*-values < 0.05 indicate that the line of best fit slope values for recent collected samples are significantly different and are lower than those of older collected samples in the last 10, 15, and 20 years of sample time series.

Supplementary Figures

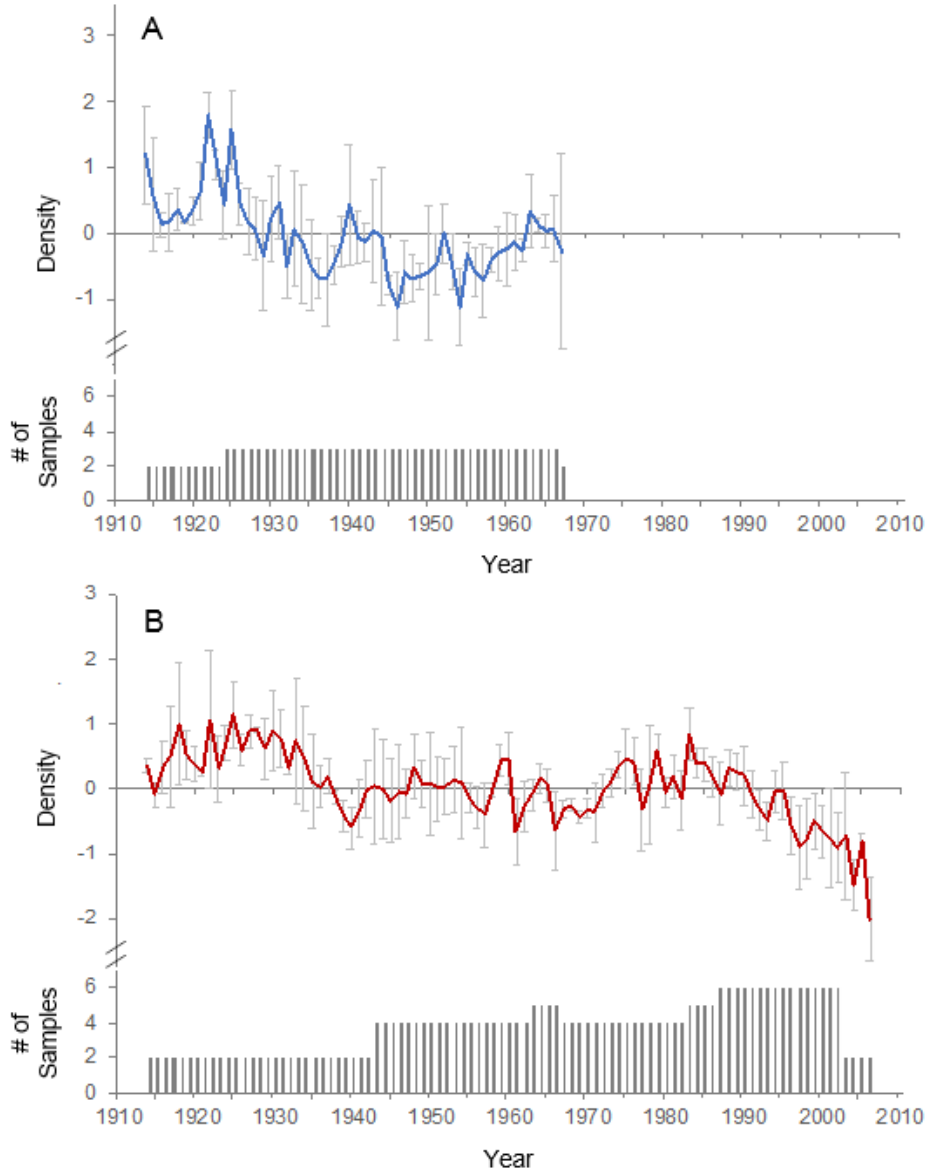

Figure DR1. Comparison of older vs. recent collected algal specimens. (A) Annual skeletal density normalized with respect to the mean for older samples collected in 1969. **(B)** Annual skeletal density normalized with respect to the mean for modern collected 2004/2008 samples. Coloured lines show annual averages for old (blue) and recent (red) collected specimens, and the light grey bars represent ± 1 standard error. The bars on the bottom of each graph indicate the number of samples averaged in each year of the time series. The upward trend in older specimens shown in the last years of growth (prior to collection) indicate the absence of an ontogenetic decline in skeletal density of coralline algae.

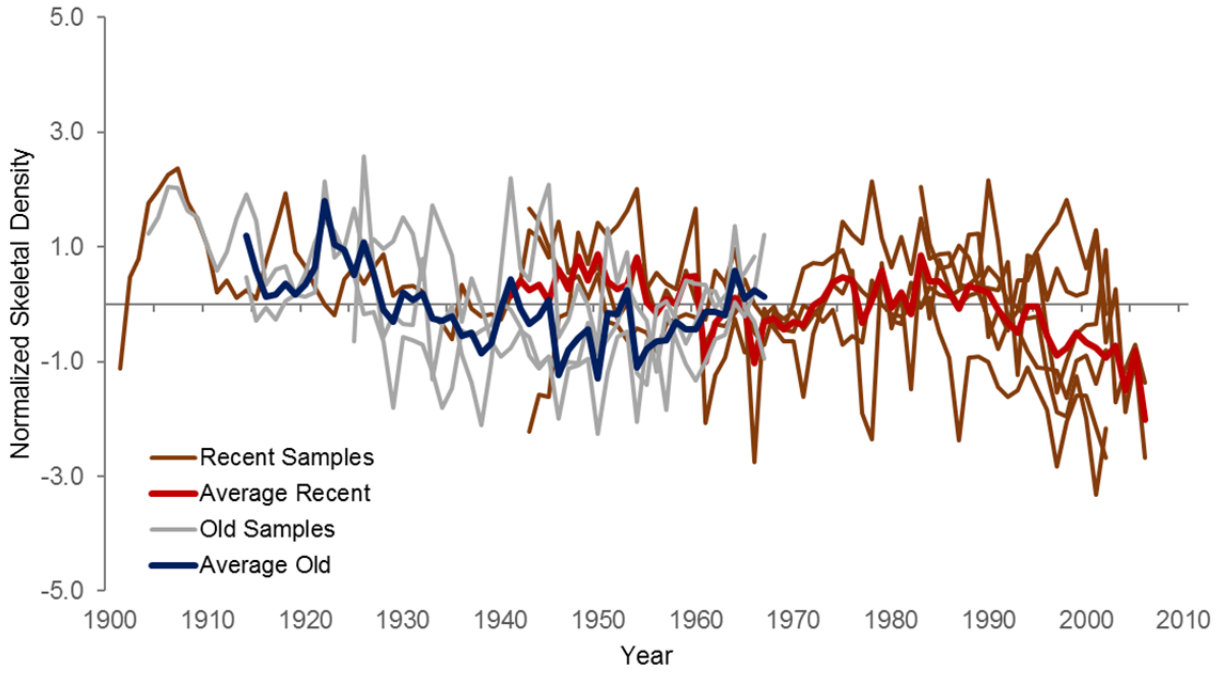

Figure DR2. Skeletal density of all samples normalized with respect to the mean. Values were normalized to highlight intraspecimen variability. Brown lines represent recent collected samples, average shown in red. Grey lines represent older collected samples, average shown in blue.

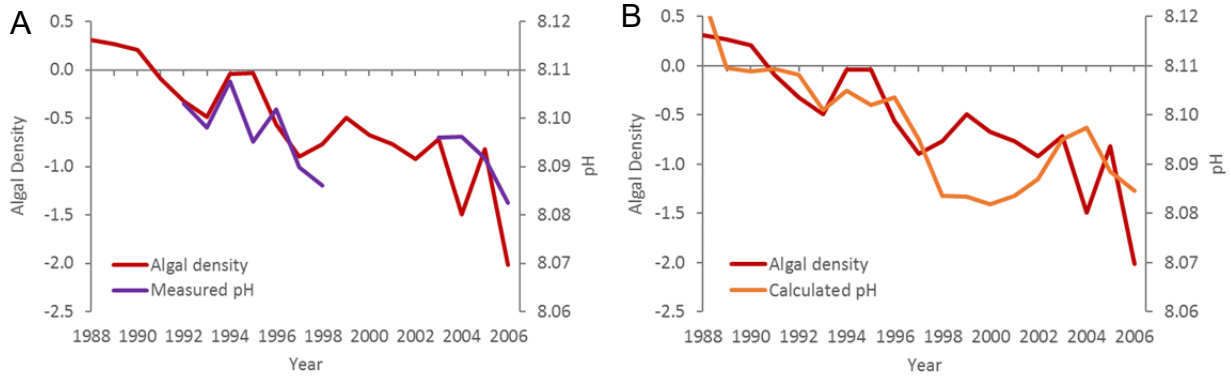

Figure DR3. Regression analyses between algal skeletal density and seawater pH. Relationship between annually resolved algal skeletal density and **(A)** mean *in-situ* measured pH at 25 °C (n = 11, r = 0.70, p = 0.016); and **(B)** mean seawater pH calculated from DIC and TA at 25 °C (n = 19, r = 0.70, p = 0.0008) from the Hawaii Ocean Time-series surface CO_2 system data

product (Dore et al., 2009). Both show a significant positive correlation such that decreasing ocean pH is associated with declining algal density.

REFERENCES CITED

Chan, P., Halfar, J., Norley, C.J.D., Pollmann, S.I., Adey, W., and Holdsworth, D.W., 2017, Micro-computed tomography: Applications for high-resolution skeletal density determinations: An example using annually banded crustose coralline algae: Geochemistry, Geophysics, Geosystems, v. 18, p. 3542-3553, doi: 10.1002/2017GC006966.

De'ath, G., Fabricius, K., and Lough, J., 2013, Yes—Coral calcification rates have decreased in the last twenty-five years!: Marine Geology, v. 346, p. 400-402, doi: 10.1016/j.margeo.2013.09.008.

D'Olivo, J.P., McCulloch, M.T., and Judd, K., 2013, Long-term records of coral calcification across the central Great Barrier Reef: assessing the impacts of river runoff and climate change: Coral Reefs, v. 32, p. 999-1012, doi: 10.1007/s00338-013-1071-8.

Dore, J.E., Lukas, R., Sadler, D.W., Church, M.J., and Karl, D.M., 2009, Physical and biogeochemical modulation of ocean acidification in the central North Pacific: Proceedings of the National Academy of Sciences of the United States of America, v. 106, p. 12235-12240, doi: 10.1073/pnas.0906044106.

Hetzinger, S., Halfar, J., Kronz, A., Steneck, R.S., Adey, W., Lebednik, P.A., and Schone, B.R., 2009, High-resolution Mg/Ca ratios in a coralline red alga as a proxy for Bering Sea temperature variations from 1902 to 1967: Palaios, v. 24, p. 406-412, doi: 10.2110/palo.2008.p08-116r.

Ridd, P.V., da Silva, E.T. and Stieglitz, T., 2013, Have coral calcification rates slowed in the last twenty years?: Marine Geology, v. 346, p. 392-399, doi: 10.1016/j.margeo.2013.09.002.